ERDC/TN EQT-16-2
August 2016

US Army Corps of Engineers®

Verification and Evaluation of Aquatic Contaminant Simulation Module (CSM)

by Zhonglong Zhang and Billy E. Johnson

PURPOSE: The United States Army Engineer Research and Development Center (ERDC) developed the aquatic contaminant simulation module (CSM). The overall purpose of the CSM is to provide a "plug in" contaminant simulation module for existing hydrologic and hydraulic (H&H) models. The CSM computes internal source and sinks for a wide range of contaminants for both water column and underlying sediment layer. Likewise, it was written as a dynamic link library (DLL) and compiled as CSM.dll. The CSM is independent of the dimensionality of the spatial domain and has general applicability to aquatic systems. In addition, it has been integrated into the Hydrologic Engineering Center-River Analysis System (HEC-RAS) (HEC 2010a, b) and Soil and Water Assessment Tool (SWAT) (Arnold et al. 1998, Neitsch et al. 2011). It will also be integrated into ERDC's Adaptive Hydraulics (AdH) model (Berger et al. 2012).

The CSM has been verified and evaluated through a series of test cases. In these tests, CSM computed results were compared to observed data available in published literatures and similar outputs generated from the RECOVERY model (Boyer et al. 1994, Ruiz et al. 2000) and Water-quality Analysis Simulation Program (WASP) model (Wool et al. 2006). This technical note (TN) describes the results of the model verification and evaluation studies. Likewise, this TN also provides information about the CSM parameter inputs and capabilities.

BRIEF DESCRIPTION OF CONTAMINANT SIMULATION MODULE (CSM): The CSM was designed to compute kinetics of contaminants in aquatic systems. Figure 1 depicts the conceptual representation of a contaminant kinetics modeled in CSM. The model domain is conceptualized as a well-mixed water column underlain by an active sediment layer. Each chemical species in the water column is subject to adsorption and desorption. In CSM, the truly dissolved phase in bulk water (aqueous phase), sorbed phase to dissolved organic carbon (DOC), algae, and sorbed phases to solids are modeled for the water column. Solid particles consist of an inorganic fraction (e.g., silts, and clays) and an organic fraction (e.g., algae, zooplankton, bacteria, and detritus). Natural waters can contain a mixture of solid particles ranging from gravel (2 mm to 20 mm) or sand (0.07 mm to 2 mm) down to very small particles classified as silt or clay (smaller than 0.07 mm). The fine fraction of solids is characterized as cohesive sediment. From a water quality perspective, cohesive sediments are usually of greater importance in water quality modeling. The chemical species in the active sediment layer is also partitioned into corresponding forms: truly dissolved phase in the pore water, sorbed phase to DOC in the pore water, and sorbed phase to the sediments. Suspended solids and underlying sediments have two types of partitioning options: equilibrium and non-equilibrium. The air compartment can be considered a sink for volatile contaminants. In CSM, contaminants can enter the water column via surface runoff, atmospheric deposition, and/or direct discharge. Once contaminants are in aquatic systems, they may be degraded or transformed by various processes

shown in Figure 1. The following processes are modeled in CSM: ionization, multi-phase partitioning, degradation, photolysis, hydrolysis, volatilization, generalized second-order reaction and transformations. The relative importance of each of the processes is directly governed by the contaminant species and their properties. The theory and mathematical formulations included in CSM can be found in Zhang and Johnson (2016).

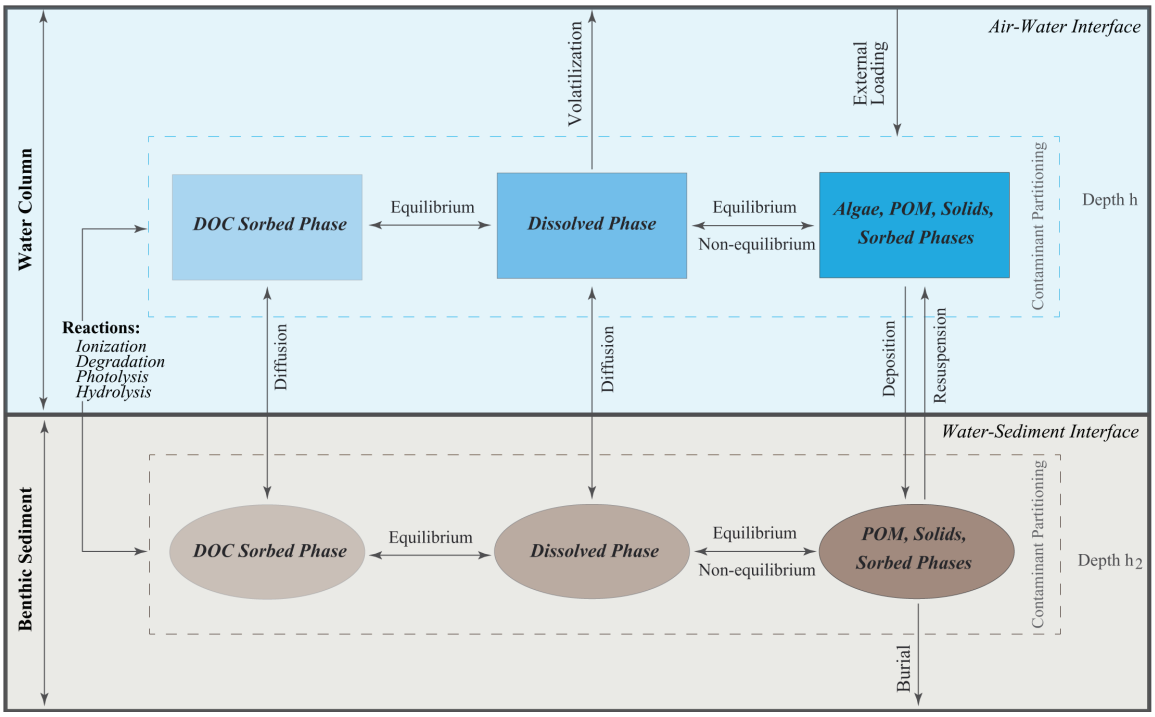

Figure 1. Conceptual representation of contaminant processes modeled in CSM.

In CSM, the sediment layer represents the upper mixed layer and may be on the order of several centimeters thick due to bioturbation and mixing. The mass balance of contaminants must be tracked for the sediment layer in the underlying water column. The sediment layer in CSM is assumed as homogeneous (i.e., well mixed), and the model does not change the thickness of sediment layer during the simulation. As the sediment layer accepts a new sediment increment on the top, an equal amount is removed from the sediment layer for burial. When sediment re-suspension occurs, it is assumed that deeper sediments below this sediment layer are entrained into the upper layer and then mixed with the remaining sediments. The density of the sediment layer can vary depending on the variable sediment composition. The porosity within the sediment layer is assumed constant and user defined. Concentrations of the contaminant computed in CSM for the sediment layer include dissolved, DOC sorbed, particulate organic matter (POM), and solids sorbed phases. All concentrations in source and sink term equations in CSM, including those for sediment contaminants, are expressed in terms of mass per unit volume of water plus solids ($\mu g\ L^{-1}$). This method is more amenable to integration with H&H transport models, for which the common concentration units are mass per unit volume. Table 1 lists the CSM's output concentrations for each contaminant.

Table 1. Computed concentrations of each contaminant in CSM.		
Name	**Definition**	**Units**
Water column		
C_T	Total concentration in water	μg L^{-1}
C_{ion}	Ionic concentration in water	μg L^{-1}
C_d	Concentration of dissolved phase in water	μg L^{-1}
C_{doc}	Concentration of DOC sorbed phase in water	μg L^{-1}
C_{ap}	Concentration of algae sorbed phase in water	μg L^{-1}
C_{pom}	Concentration of POM sorbed phase in water	μg L^{-1}
C_{pt}	Total concentration of solids sorbed phase in water	μg L^{-1}
C_{pts}	Total concentration of solids sorbed phase in water	μg g^{-1}
Sediment layer		
C_{T2}	Total concentration in sediment	μg L^{-1}
C_{ion2}	Ionic concentration in water	μg L^{-1}
C_{d2}	Concentration of dissolved phase in pore water	μg L^{-1}
C_{doc2}	Concentration of DOC sorbed phase in pore water	μg L^{-1}
C_{pom2}	Concentration of POM sorbed phase in sediment	μg L^{-1}
C_{pt2}	Total concentration of solids sorbed phase in sediment	μg L^{-1}
C_{pts2}	Total concentration of solids sorbed phase in sediment	μg g^{-1}

VERIFICATION STUDIES: An important category of a newly developed CSM includes the algorithm tests normally associated with verification of computer codes. Algorithm tests serve multiple purposes. They are intended, in part, to discover bugs and, in part, to verify the merit of the algorithm to solve the problems. Therefore, we conducted a set of model testing cases to verify the CSM and evaluate the model performance. The CSM was first verified against field-scale experiment data included in the RECOVERY model (Boyer et al. 1994). The benefits of CSM field verification efforts are significant, including confirming the CSM to field conditions. Since the key kinetic algorithms in CSM are adopted from the WASP model, results generated from WASP were used to verify the CSM. The CSM and WASP models were run with a consistent set of kinetic coefficients and parameters and initial conditions in all test cases. In addition, non-linear and non-equilibrium sorptions can be modeled in CSM for algae, POM, and solids, but these mechanisms are not included in the WASP model. Therefore, the CSM was further tested and evaluated through several special cases and sensitivity analysis.

Field Data Verification. The CSM was used to analyze a field-scale experiment in which a flooded limestone quarry was treated with equal amounts of the insecticides Dichlorodiphenyldichloroethylene (DDE) and lindane. The study was conducted in two flooded limestone quarries (T and C) located near the town of Oolitic in Bedford County, IN. The quarries were allowed to flood naturally for five years before being dosed with DDE and lindane. Quarry T was the smaller of the two in area, with extremely clear water and generally flat bottom. Quarry T was 91.4 m long, 41.1 m wide, and an average of 15.2 m deep. The water depth in the quarry was 13.9 m. The average Secchi disc reading for quarries C and T was 20 ft. Both quarries exhibited thermal stratification from March to November. The bottom material in quarry T was made up of 3 to 5 cm of fine brownish gyttja underlain by a white inorganic mixture of limestone dust and silica sand. In general, the top sediment layers were aerobic, while the mud layer contained, on average, 1% sand, 42% silt, and 57% clay.

Quarry T was treated with DDE and lindane at a concentration of 200 ppt to the epilimnion or 50 ppt overall (2.7764 g of DDE and 2.7752 g of lindane) (Waybrant 1973). The quarries were analyzed after the treatment, and the results showed that essentially all of the insecticides were initially released in the epilimnion. The quarries were periodically sampled, and both water and bottom sediments were analyzed for DDE and lindane. The detailed data used in this test case is available in Di Toro and Paquin (1982) and Boyer et al. (1994). This experiment was previously analyzed with the RECOVERY model. The RECOVERY model results for DDE and lindane in the water column and bottom sediment material were provided in Boyer et al. (1994) and Ruiz et al. (2000).

Initial water concentration for DDE was set to $3.5 \cdot 10^{-3}$ µg L^{-1} and $2.54 \cdot 10^{-2}$ µg L^{-1} for lindane. The initial sediment concentration was set to $3.53 \cdot 10^{-2}$ µg L^{-1} for DDE and $1.87 \cdot 10^{-3}$ µg L^{-1} for lindane. Suspended solids were set to 5 mg L^{-1}. Resuspension was set to zero, and the burial velocity was set to $5.0 \cdot 10^{-4}$ m $year^{-1}$. Di Toro and Paquin (1982) indicated that the inflow to the quarry was assumed to be insignificant in comparison to the overall volume of water in the quarry, so inflow loads are ignored in CSM simulation. The settling velocity was set to 87.5 m $year^{-1}$, which was estimated from the solids mass balance in RECOVERY (Boyer et al. 1994). In addition to sedimentation processes (i.e., settling and burial), kinetic processes modeled for DDE and lindane included partitioning, degradation, and volatilization. Table 2 provides a summary of DDE and lindane parameters used in this verification study. Other parameters for DDE and lindane were provided in Boyer et al. (1994).

Table 2. Summary of DDE parameters used in the CSM verification.

Variable	Definition	Value	Units
v_s	Settling velocity	0.24	m d^{-1}
v_b	Burial velocity	$5.0 \cdot 10^{-4}$	m yr^{-1}
MW	Molecular weight	354.6	g mol^{-1}
D_m	Molecular diffusivity	$5.0 \cdot 10^{-6}$	cm^2 s^{-1}
v_m	Sediment-water mass transfer velocity	$1.37 \cdot 10^{-6}$	cm s^{-1}
h_2	Sediment layer thickness	0.01	m
Equilibrium partitioning			
K_{ow}	Octanol-water partitioning coefficient	$5.0 \cdot 10^4$	-
K_p	Equilibrium partition coefficient for solids in water	$1.54 \cdot 10^3$	L kg^{-1}
f_{oc}	Fraction of organic carbon in suspended solids	0.05	-
K_{p2}	Equilibrium partition coefficient for solids in sediments	$1.54 \cdot 10^3$	L kg^{-1}
f_{oc2}	Fraction of organic carbon in sediment solids	0.05	-
Volatilization			
v_v	Volatilization velocity	0.14058	m d^{-1}
K_H	Henry's constant	$3.9 \cdot 10^{-5}$	atm m^3 (g mol $^oK)^{-1}$
K_G	Mass transfer velocity from the gaseous film	58213	m d^{-1}
K_L	Mass transfer velocity from the liquid film	108.9	m d^{-1}

The information in Tables 2 and 3 was used to fill out the Input Parameters from the CSM user interface. The CSM was setup to simulate DDE and lindane for a 10 year period. Excluding adjustments made for the sediment-water transfer velocity, minimum calibration was performed during verification. The total concentrations, dissolved, and solid sorbed phases of DDE and lindane in the

water column and upper sediment layer were reported in model outputs. The CSM simulation results were compared with observed data. The comparisons between computed CSM and observed DDE concentrations for the water column and upper sediment layer are presented in Figures 2 and 3. Major losses of DDE from the water column are caused by settling of suspended solids, attached DDE, and the volatilization process. The only removal mechanism in the sediment layer is deep burial. The sediment-water transfer flux is small. The model prediction does not represent range established for the observed data at the beginning of the simulation. The field data are strongly subject to daily fluctuations, which affect the simulation for DDE with the calibrated parameters where the same region presents DDE in accordance with the trend observed for DDE. Despite the variability in measured data, modeled DDE values captured the major trends of DDE temporal variation in both water column and sediment layer. A strong indication of the model prediction with the observed data is found after five years. Computed DDE in the water column agrees very well with the observed concentration of less than $1 \cdot 10^{-3}$ µg L^{-1}. The CSM over-predicts the DDE concentration of 5.6 µg L^{-1} in the upper sediment layer after five years. Likewise, the RECOVERY model also produced similar results (Boyer et al. 1994).

Table 3. Summary of lindane parameters used in the CSM verification.

Variable	Definition	Value	Units
v_s	Settling velocity	0.1	m d^{-1}
v_b	Burial velocity	$2.1 \cdot 10^{-4}$	m yr^{-1}
MW	Molecular weight	290	g mol^{-1}
D_m	Molecular diffusivity	$5.0 \cdot 10^{-6}$	cm^2 s^{-1}
v_m	Sediment-water mass transfer velocity	$1.37 \cdot 10^{-6}$	cm s^{-1}
h_2	Sediment layer thickness	0.03	m
Equilibrium partitioning			
K_{ow}	Octanol-water partitioning coefficient	$5.01 \cdot 10^3$	-
K_p	Equilibrium partition coefficient for solids in water	$1.54 \cdot 10^2$	L kg^{-1}
f_{oc}	Fraction of organic carbon in suspended solids	0.05	-
K_{p2}	Equilibrium partition coefficient for solids in sediments	$1.54 \cdot 10^2$	L kg^{-1}
f_{oc2}	Fraction of organic carbon in sediment solids	0.05	-
Degradation			
n	Degradation order in water	1	-
k_d	Degradation rate for dissolved phase in water	0.9	d^{-1}
k_p	Degradation rate for solids sorbed phase in water	0.0	d^{-1}
n	Degradation order in sediment	1	-
k_d	Degradation rate for dissolved phase in sediment	0.9	d^{-1}
k_p	Degradation rate for solids sorbed phase in sediment	0.0	d^{-1}
Volatilization			
v_v	Volatilization velocity	0.0018	m d^{-1}
K_H	Henry's constant	$4.9 \cdot 10^{-7}$	atm m^3 (g mol $^oK)^{-1}$
K_G	Mass transfer velocity from the gaseous film	31831	m d^{-1}
K_L	Mass transfer velocity from the liquid film	95.3	m d^{-1}

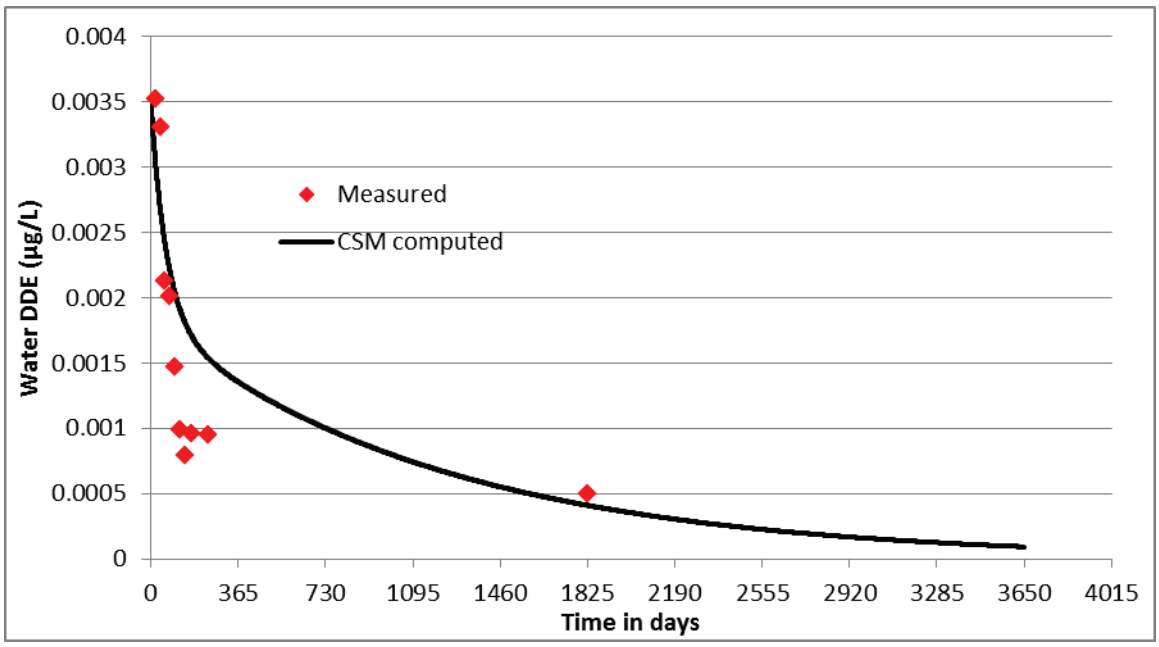

Figure 2. Comparison of CSM computed and measured concentrations of DDE in the water column.

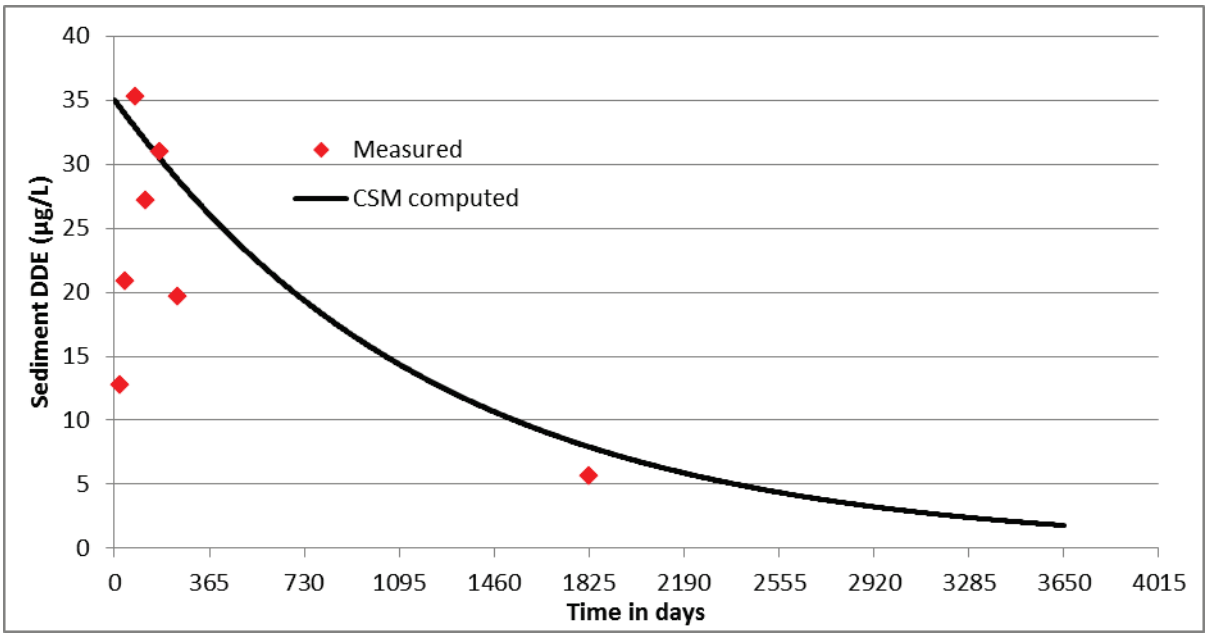

Figure 3. Comparison of CSM computed and measured concentrations of DDE in the upper sediment layer.

Figues 4 and 5 show the comparison of CSM computed and observed lindane concentrations in the water column and sediment layer. Concentrations of lindane decrease more quickly than DDE due to additional degradation. Lindane decreases from initial 0.025 µg L^{-1} in the water column and 1.8 µg L^{-1} in the upper sediment layer to almost zero after five years. Besides the volatilization, its degredation is the major mechanism for the decrease from the water column. This field verification and

comparison against the field observed data shows the ability of the CSM to simulate behavior of two insecticides in an aquatic system with a limited amount of data. CSM computed results are similar to those predicted by the RECOVERY model, thus, appear to demonstrate the validity of the algorithms used to describe the kinetics and fate of insecticides in the water column and underlying sediments.

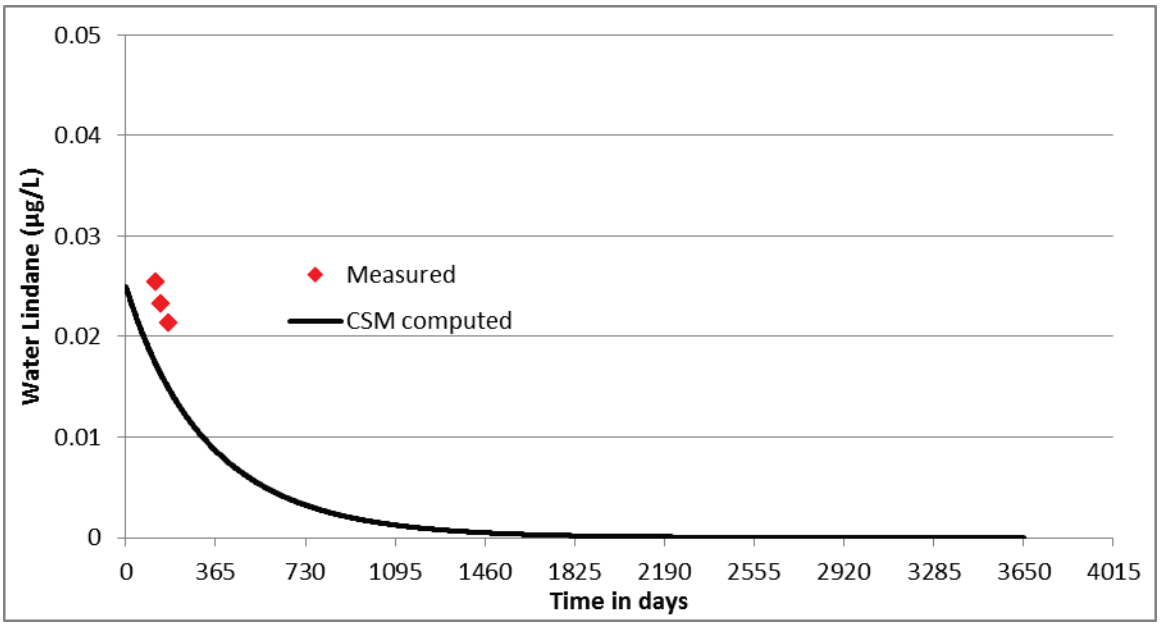

Figure 4. Comparison of CSM computed and measured concentrations of lindane in the water column.

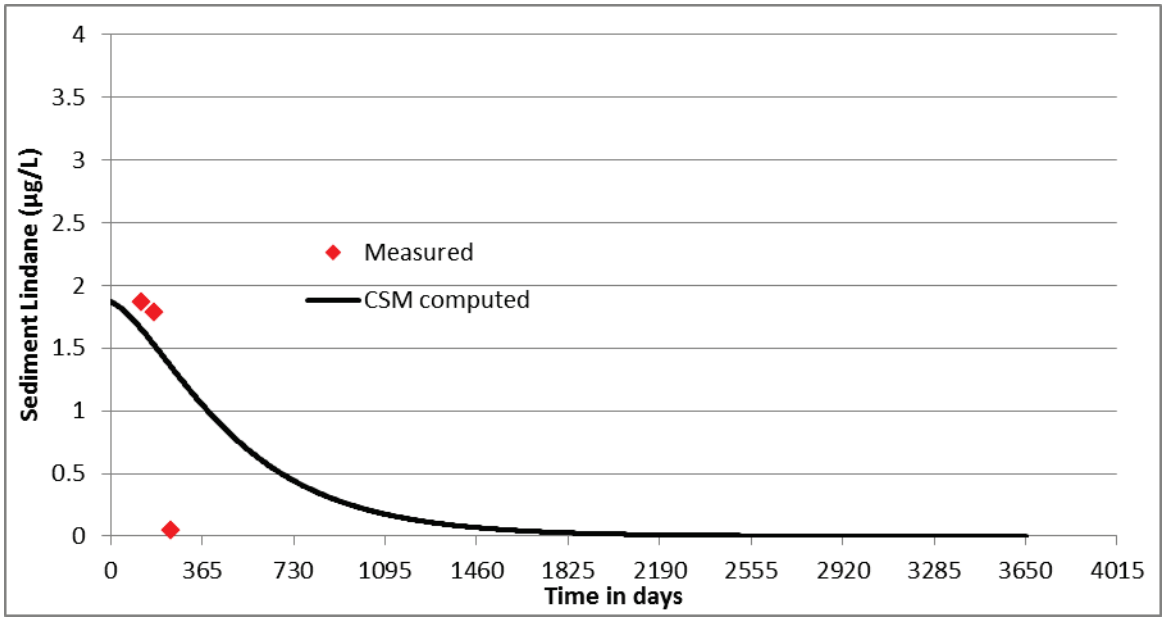

Figure 5. Comparison of CSM computed and measured concentrations of lindane in the upper sediment layer.

Comparison of CSM and WASP Model Simulations. In this test case, an equivalent water column and benthic sediment segment was set up for CSM and WASP simulations. Each model ran for a period of 1000 days. The concentrations and pathway fluxes of contaminants computed by the CSM were compared against their values generated from the WASP simulation. Three contaminants named as Chem 1, Chem 2, and Chem 3 were simulated for each model. The diffusion velocity between the water column and underlying sediment-water was set to zero because this process, included in WASP, did not behave appropriately. Different kinetic processes for each contaminant were simulated to validate CSM performance against corresponding WASP simulation for each contaminant during this test case. Three species of contaminants and two solids classes were simulated in both models.

The first two contaminants (Chem 1 and Chem 2) represent two insecticides thiometon and disulfoton. Wanner et al. (1989) performed a detailed modeling study for the transport and fate of these two compounds at the Rhine River in Schweizerhalle, Switzerland. A dynamic mathematical model was developed to predict the propagation and attenuation of the pulse of the two chemicals in the Rhine River. The internal processes modeled in their study include sorption and settling, diffusion into sediments, water/air exchange, as well as chemical, photochemical, and biological transformations. In their study, abiotic hydrolysis and biological transformation of thiometon and disulfoton have been measured in laboratory experiments. Their laboratory data, together with estimates based on available data, were used in CSM and WASP simulations. The detailed data used for these two compounds is available in Wanner et al. (1989). Because some kinetic processes were not simulated for these two compounds, a third contaminant, which is an arbitrary chemical used to test and validate contaminants kinetics not simulated for thiometon and disulfoton, was included in this case study.

Multi-phase partition to DOC, POM, and two solid classeses were allowed for the third contaminant. The three contaminants were also subject to several reactions and transformations, including degradation, hydrolysis, phololysis, generalized second-order reaction, transformations in the water column and sediment layer, and volatilization of contaminants in the water column. These simulations assumed that solid 1 and solid 2 settle out at a velocity of 1.0 and 5.0 m/day. Solid 1 and solid 2 in the surficial sediment compartments were assumed to resuspend at a velocity of 0.01 and 0.05 m/day, respectively. Sediment burial rate was setup as 0.0002 m/day. The exchanging solids carry sorbed contaminants between the water column and surficial sediment. Table 4 presents the values of the contaminant parameters used in these two models.

Biochemical processes simulated for Chem 1 included contaminant partitioning (five phases), degradation, photolysis, volatilization, and transformations due to the degradation. In this test case, equilibrium partitioning coefficients for DOC, POM, and solids were selected as user specified parameters in both models. Volatilization velocity of Chem 1 was internally computed in both models. Comparisons of CSM and WASP model computed concentrations of Chem 1 in the water column and sediment layer are shown in Figures 6 and 7. Total and dissolved concentrations are presented for the water column. Total concentration and sorbed mass on sediment solids are presented for the sediment layer. The CSM and WASP produced identical results as expected because the same biochemical reactions and transformation mechanisms and rates were applied both models. Examination of Figure 6 reveals that the dissolved concentration contains a significant portion of the total concentration in the water column.

Table 4. Summary of contaminant parameters used in CSM and WASP simulations.

Variable	Definition	Value	Temp. Coeff.	Value	Temp. Coeff.	Value	Temp. Coeff.	Units
		Chem 1 (Disulfoton)		Chem 2 (Thiometon)		Chem 3		
MW	Molecular weight	200						g mol^{-1}
h_2	Sediment layer thickness	0.15		0.15	-	0.15	-	m
v_m	Sediment-water mass transfer velocity	0		0	-	0	-	m d^{-1}
K_{ow}	Octanol-water partitioning coefficient	-	-	-	-	100000	-	-
α_{doc}	Partition correlation coefficient	-	-	-	-	0.65	-	-
α_{pom}	Partition correlation coefficient	-	-	-	-	0.65	-	-
α_p	Partition correlation coefficient	-	-	-	-	0.65	-	-
K_{doc}	Equilibrium partition coefficient for DOC	1500		250	-	65000	-	L kg^{-1}
K_{doc2}	Equilibrium partition coefficient for DOC	1500		250	-	65000	-	L kg^{-1}
K_{pom}	Equilibrium partition coefficient for POM	1200		240	-	-	-	L kg^{-1}
K_{pom2}	Equilibrium partition coefficient for POM	1200		240	-	-	-	L kg^{-1}
K_{p_1}	Equilibrium partition coefficient for solid 1	500		120	-	-	-	L kg^{-1}
K_{p2_1}	Equilibrium partition coefficient for solid 1	500		120	-	-	-	L kg^{-1}
K_{p_2}	Equilibrium partition coefficient for solid 2	300		60	-	-	-	L kg^{-1}
K_{p2_2}	Equilibrium partition coefficient for solid 2	300		60	-	-	-	L kg^{-1}
n	Degradation order	1		-	-	-	-	-
k_{1d}	Degradation rate for dissolved phase in water	0.005	1.025	-	-	-	-	d^{-1}
k_{1d2}	Degradation rate for dissolved phase in sediment	0.005	1.025	-	-	-	-	d^{-1}
k_{1doc}	Degradation rate for DOC sorbed phase in water	0.002	1.025	-	-	-	-	d^{-1}
k_{1doc2}	Degradation rate for DOC sorbed phase in sediment	0.002	1.025	-	-	-	-	d^{-1}
k_{1pom}	Degradation rate for POM sorbed phase in water	0.001	1.025	-	-	-	-	d^{-1}
k_{1pom2}	Degradation rate for POM sorbed phase in sediment	0.001	1.025	-	-	-	-	d^{-1}
k_{1p}	Degradation rate for solids sorbed phase in water	0.001	1.025	-	-	-	-	d^{-1}
k_{1p2}	Degradation rate for solids sorbed sorbed phase in sediment	0.001	1.025	-	-	-	-	d^{-1}
Y_{12}	Transformation yield coefficient from chemical 1 to 2	0.2		-	-	-	-	-

Y_{12}	Transformation yield coefficient from chemical 1 to 2	0.3		-	-	-	-	-
k_{pht}	Aquatic photolysis rate for dissolved phase	0.00752	-	-	-	-	-	d^{-1}
k_{phtdoc}	Aquatic photolysis rate for DOC sorbed phase	0.00376	-	-	-	-	-	d^{-1}
I_{0pht}	Light intensity when k_{pht} is measured	200	-	-	-	-	-	W m^{-2}
v_v	Volatilization velocity	2	1.025	-	-	-	-	m d^{-1}
K_H	Henry's constant	$2.5 \cdot 10^{-3}$	$5.0 \cdot 10^{-4}$	-	-	-	-	atm L mol^{-1}
k_{hb}	Alkaline hydrolysis rate of dissolved phase in water	-	-	2	-	-	-	m^3 mol^{-1} d^{-1}
k_{hb2}	Alkaline hydrolysis rate of dissolved phase in sediment	-	-	2	-	-	-	m^3 mol^{-1} d^{-1}
k_{hbdoc}	Alkaline hydrolysis rate of DOC sorbed phase in water	-	-	1	-	-	-	m^3 mol^{-1} d^{-1}
k_{hbdoc2}	Alkaline hydrolysis rate of DOC sorbed phase in sediment	-	-	1	-	-	-	m^3 mol^{-1} d^{-1}
E_{ahb}	Activation energy for alkaline hydrolysis	-	-	65	-	-	-	KJ mol^{-1}
k_{hn}	Neutral hydrolysis rate of dissolved phase in water	-	-	0.00013	-	-	-	d^{-1}
k_{hn2}	Neutral hydrolysis rate of dissolved phase in sediment	-	-	0.00013	-	-	-	d^{-1}
k_{hndoc}	Neutral hydrolysis rate of DOC sorbed phase in water	-	-	0.00006	-	-	-	d^{-1}
k_{hndoc2}	Neutral hydrolysis rate of DOC sorbed phase in sediment	-	-	0.00006	-	-	-	d^{-1}
E_{ahn}	Activation energy for neutral hydrolysis	-	-	76	-	-	-	KJ mol^{-1}
k_{ha}	Acid hydrolysis rate of dissolved phase in water	-	-	10	-	-	-	m^3 mol^{-1} d^{-1}
k_{ha2}	Acid hydrolysis rate of dissolved phase in sediment	-	-	10	-	-	-	m^3 mol^{-1} d^{-1}
k_{hadoc}	Acid hydrolysis rate of DOC sorbed phase in water	-	-	5	-	-	-	m^3 mol^{-1} d^{-1}
k_{hadoc2}	Acid hydrolysis rate of DOC sorbed phase in sediment	-	-	5	-	-	-	m^3 mol^{-1} d^{-1}
E_{aha}	Activation energy for acid hydrolysis	-	-	65	-	-	-	KJ mol^{-1}
Tr_{hyd}	Reference water temperature for hydrolysis	-	-	24	-	-	-	°C
k_{ed}	Second-order rate for dissolved phase in water	-	-	-	-	0.001	-	$(mg\ L^{-1})^{-1}$ d^{-1}
k_{edoc}	Second-order rate for DOC sorbed phase in water	-	-	-	-	0.0008	-	$(mg\ L^{-1})^{-1}$ d^{-1}
k_{epom}	Second-order rate for POM sorbed phase in water	-	-	-	-	0.0006	-	$(mg\ L^{-1})^{-1}$ d^{-1}
k_{ep}	Second-order rate for solids sorbed phase in water	-	-	-	-	0.0006	-	$(mg\ L^{-1})^{-1}$ d^{-1}
k_{ed2}	Second-order rate for dissolved phase in sediment	-	-	-	-	0.001	-	$(mg\ L^{-1})^{-1}$ d^{-1}

k_{edoc2}	Second-order rate for DOC sorbed phase in sediment	-	-	-	-	0.0008	-	$(mg\ L^{-1})^{-1}\ d^{-1}$
k_{epom2}	Second-order rate for POM sorbed phase in sediment	-	-	-	-	0.0006	-	$(mg\ L^{-1})^{-1}\ d^{-1}$
k_{ep2}	Second-order rate for solids sorbed phase in sediment	-	-	-	-	0.0006	-	$(mg\ L^{-1})^{-1}\ d^{-1}$
E_{ae}	Activation energy for generalized second-order reaction	-	-	-	-	83.68	-	$KJ\ mol^{-1}$
Tr_{ae}	Reference water temperature for generalized second-order reaction	-	-	-	-	24	-	°C

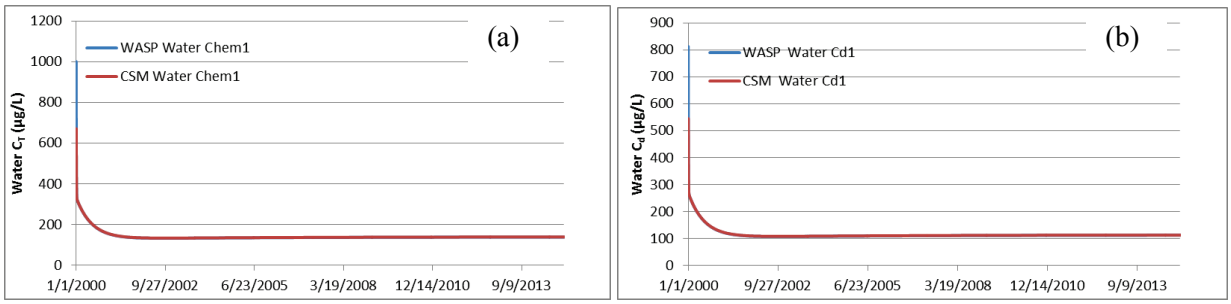

Figure 6. CSM and WASP computed concentrations of Chem 1 in the water column: (a) total (C_T) and (b) dissolved (C_d).

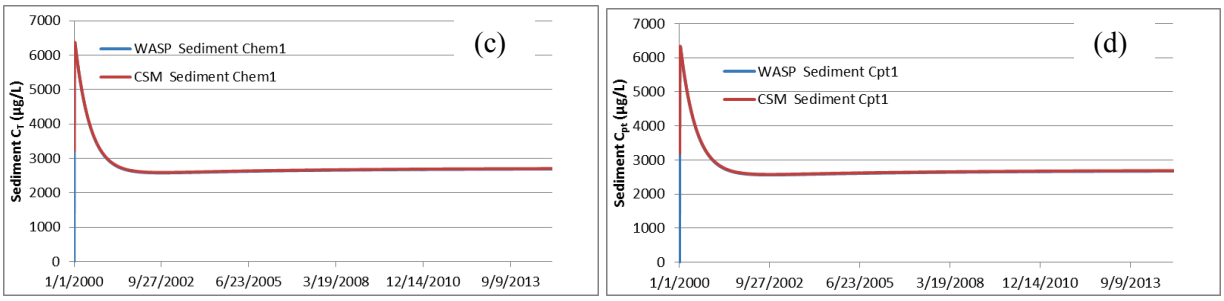

Figure 7. CSM and WASP computed concentrations of Chem 1 in the sediment layer: (a) total (C_T) and (b) solids sorbed (C_{pt}).

Biochemical processes simulated for Chem 2 include contaminant partitioning (five phases), hydrolysis, and transformation due to hydrolysis. Comparisons of CSM and WASP model computed concentrations of Chem 2 in the water column and sediment layer are shown in Figures 8 and 9. The total and dissolved concentrations of Chem 2 are presented for the water column. The CSM and WASP produced identical results, as expected, because the same biochemical reactions and transformation mechanisms and rates were applied in these two models. Among three contaminants, Chem 2 was represented with the lowest K_d value. Examination of Figure 8 reveals that the total concentration of Chem 2 is about the same magnitude as the dissolved concentration, or most of the water concentration of Chem 2 is in dissolved form because lower partitioning coefficients were specified.

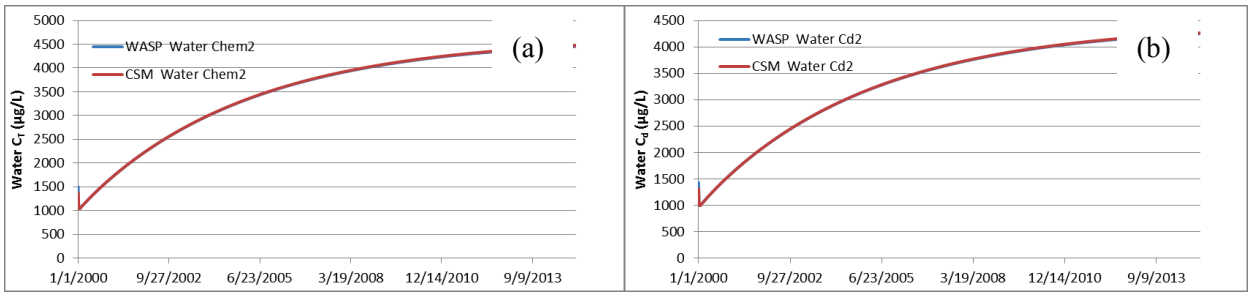

Figure 8. CSM and WASP computed concentrations of Chem 2 in the water column: (a) total (C_T) and (b) dissolved (C_d).

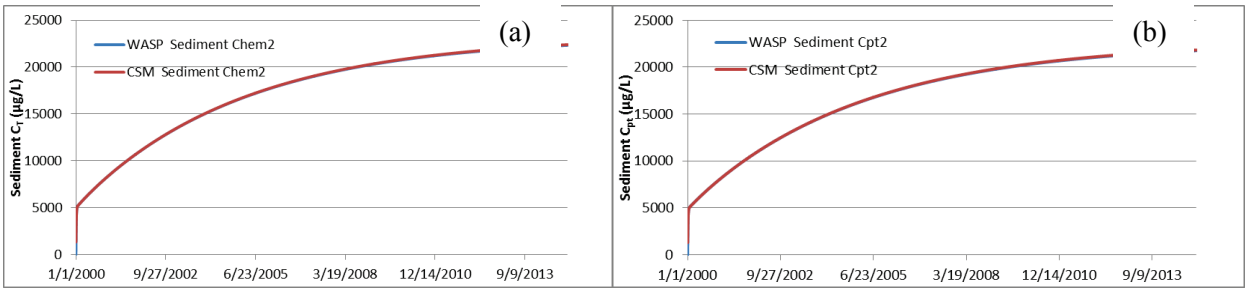

Figure 9. CSM and WASP computed concentrations of Chem 2 in the sediment layer: (a) total (C_T) and (b) solids sorbed (C_{pt}).

Biochemical processes simulated for Chem 3 include contaminant partitioning (five phases), generalized second-order reaction, and transformation due to the second-order reaction. In this test case, equilibrium partitioning coefficients for DOC, POM, and solids were computed from K_{ow} inputs instead of user specified. Comparisons of CSM and WASP computed concentrations of Chem 3 in the water column and sediment layer are shown in Figures 8 and 9. Total and dissolved concentrations are presented for the water column. The CSM and WASP produced identical results, as expected, because the same second-order reaction and transformation mechanisms and rates were applied both models. Among the three contaminants, Chem 3 was represented with the highest K_d value. Examination of Figures 9 and 10 reveals that the total concentration of Chem 3 is about several order of magnitude greater than the dissolved concentration, or most of the water concentration of Chem 3 is in particulate form (i.e., attached to solids). Chemicals with high K_d tend to be absorbed by the solids much more readily than those with low K_d.

Besides observing sediment-water fluxes computed from CSM and WASP are different, we noticed some contaminant processes included in CSM and WASP also perform differently. These differences include: (1) photolysis, (2) equilibrium partitioning coefficients computed from K_{ow}, and (3) ionization.

For the above test cases, degradation, volatilization, and all transforms were turned off for Chem 1. Only partitioning and photolysis processes were simulated in CSM and WASP. The normalized light intensity in WASP was set to equal the light intensity / reference light intensity in CSM. The model results reveal that the two models generated identical results as shown in Figure 8 if the photolysis rate for dissolved phase is specified to a no-zero value, and the photolysis rate for DOC-complex is set to zero. However, if the photolysis rate for DOC-complex is set to a no-zero value and zero for the dissolved phase, the contaminant concentrations predicted from the two models are slightly different because the computed photolysis rates were different, as shown in Figure 12.

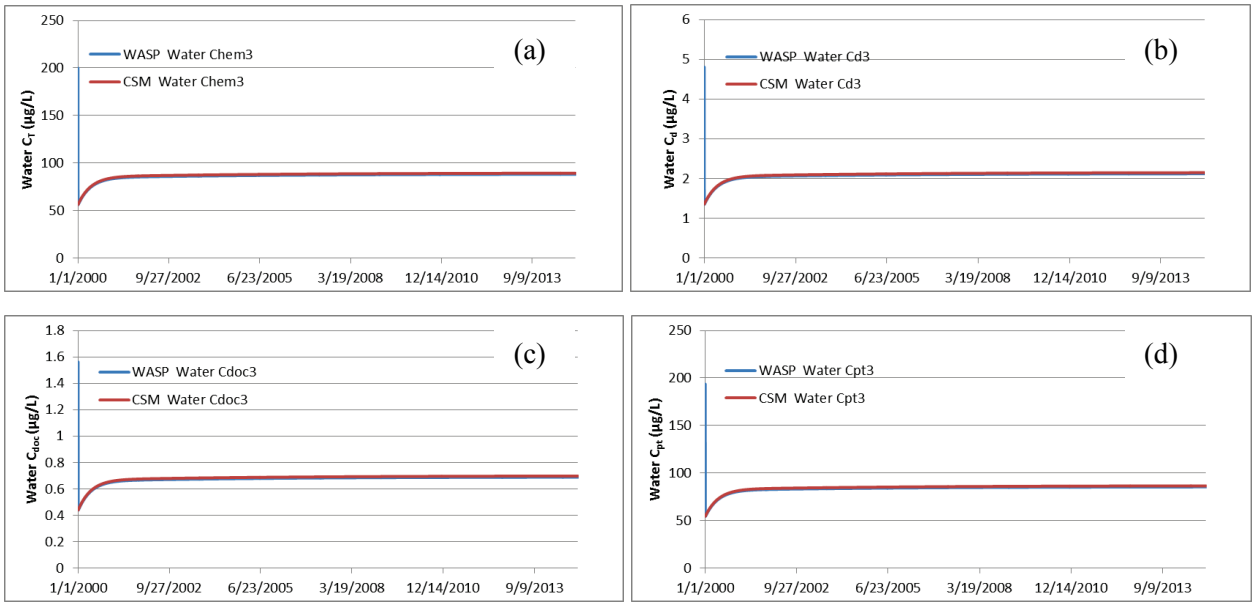

Figure 10. CSM and WASP computed concentrations of Chem 3 in the water column: (a) total (C_T), (b) dissolved (C_d), (c) DOC sorbed (C_{doc}), and (d) solids sorbed (C_{pt}).

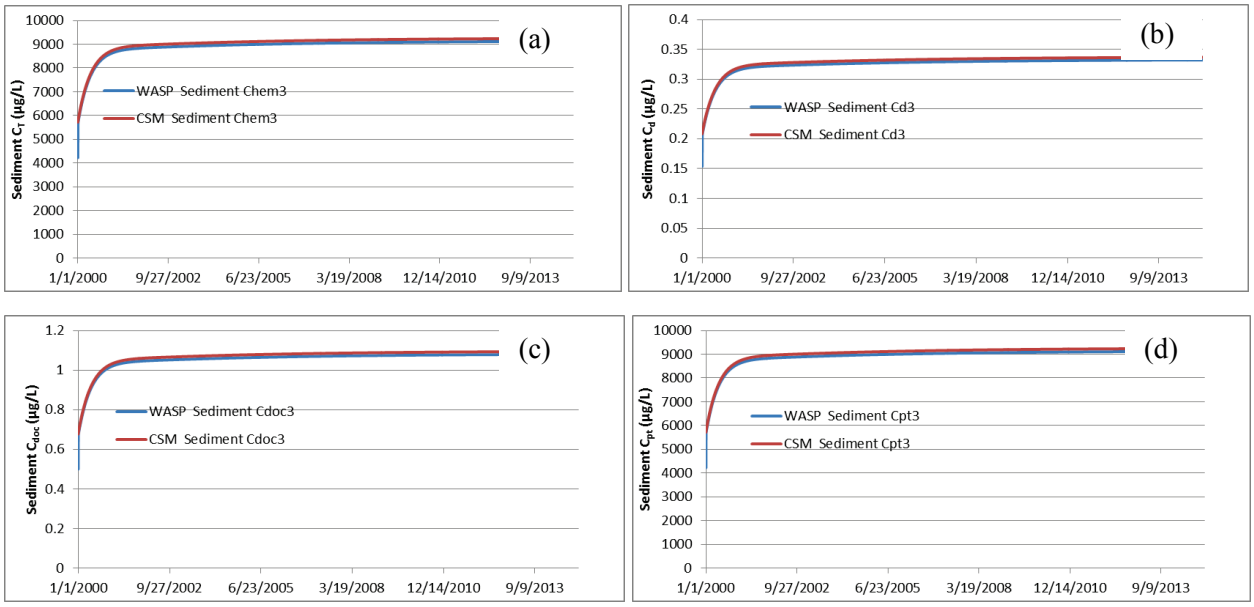

Figure 11. CSM and WASP computed concentrations of Chem 3 in the sediment layer: (a) total (C_T), (b) dissolved (C_d), (c) DOC sorbed (C_{doc}), and (d) solids sorbed (C_{pt}).

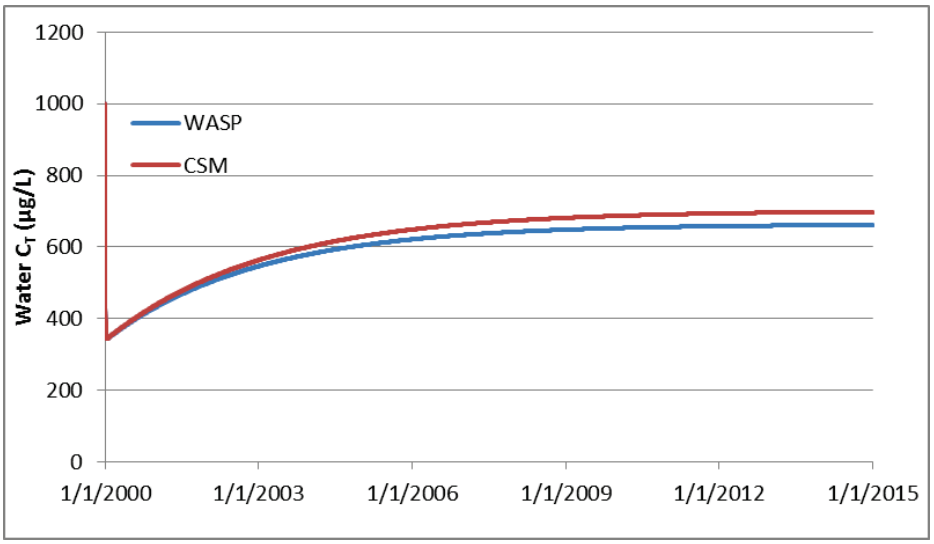

Figure 12. CSM and WASP computed total concentrations of Chem 1 in the water column.

Two options are included in CSM and WASP for defining contaminant's equilibrium partition coefficients (K_{doc}, K_{pom}, K_{pn}): (1) user-defined and (2) model computed from the octanol-water partition coefficient (K_{ow}) of the contaminant. As for the second option, different f_{oc} values for solid groups were specified in CSM and WASP, but user-specified f_{oc} values did not affect computed K_d in WASP; Therefore computed K_d values from CSM and WASP were different, which affected the model predictions.

Lastly, the ionization process in CSM and WASP behave differently. For the above test cases, ionization was turned on for Chem 3. Dissolved concentrations of Chem 3 in the water column and sediment layer are shown in Figures 13 and 14. These figures show that the dissolved concentrations computed from CSM and WASP are slightly different. Although dissolved concentrations for CSM and WASP are different, DOC and solids sorbed concentrations are approximately the same. In CSM, the contaminant is first distributed into five ionic species. Then, each species is partitioned according to its partition coefficients, which does not affect the concentration of ionic species. However, the concentration of ionic species varies with partition coefficients in WASP, resulting in different results shown in Figures 13 and 14.

Overall, CSM computed concentrations and pathway fluxes of the three contaminants were identical or slightly different compared with the corresponding results generated from the WASP model. These slight differences were largely due to some processes being implemented differently in WASP. However, the algorithm and computer code computation were implemented in CSM with confidence.

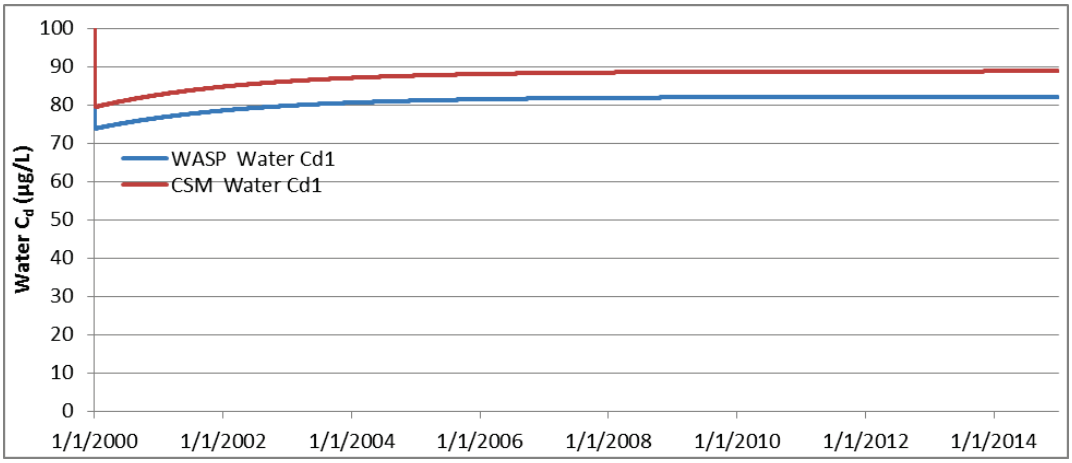

Figure 13. CSM and WASP computed dissolved concentrations of Chem 3 in the water column.

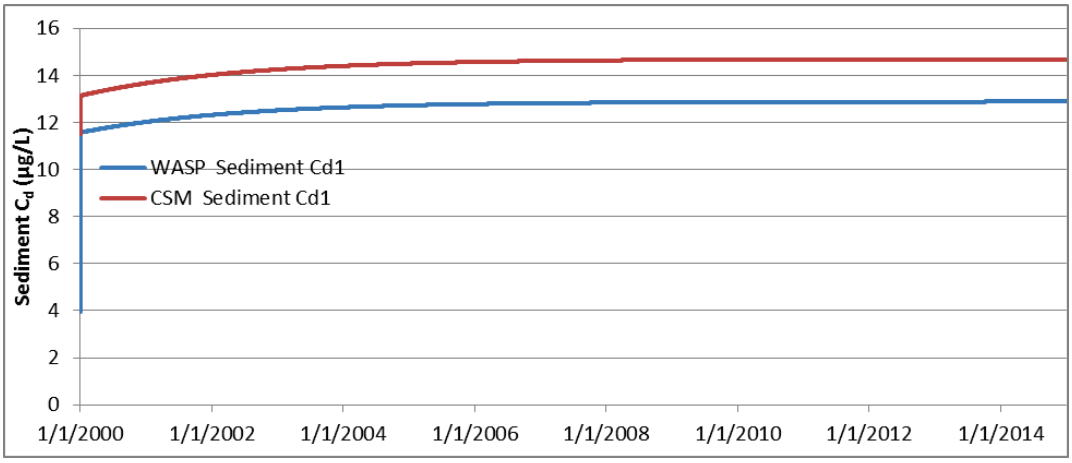

Figure 14. CSM and WASP computed dissolved concentrations of Chem 3 in the sediment layer.

ADDITIONAL VERIFICATION AND EVALUATION: A set of Microsoft Excel spreadsheets were developed to verify multiple phase partitioning, pathways, and concentrations of each phase computed in CSM. One testing case was to turn on all kinetic processes included in CSM for an arbitrary contaminant (e.g. ionization, multi-phase partitioning, degradation, photolysis, hydrolysis, volatilization, generalized second-order reaction, and transformations). Contaminant partition to DOC, algae, POM, and three solids classes were modeled for this contaminant. The dissolved species was allowed to exchange between the water column and underlying sediments through a vertical diffusion process. CSM computed concentration and pathway fluxes were identical with the results generated from source and sink term equations basedExcel spreadsheet. Comparisons of the total concentrations in the water column and sediment layer are presented in Figures 15 and 16 respectively.

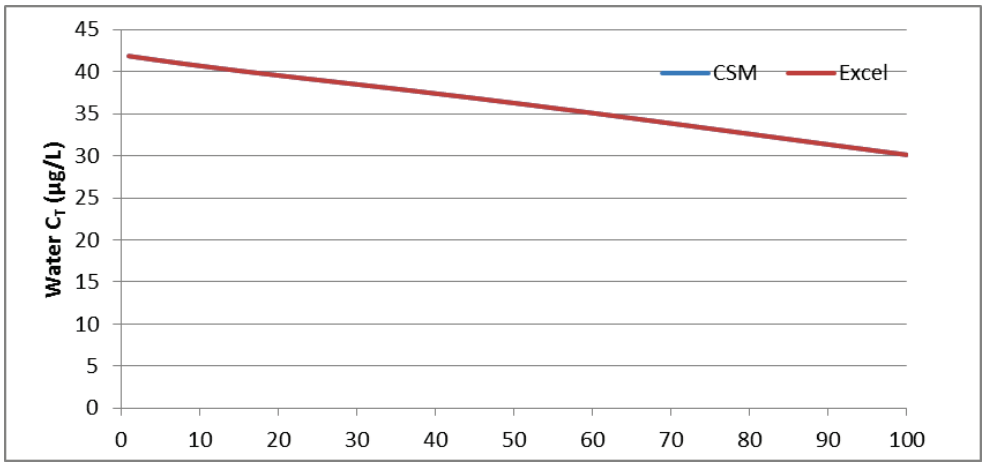

Figure 15. CSM and Excel computed total concentrations in the water column.

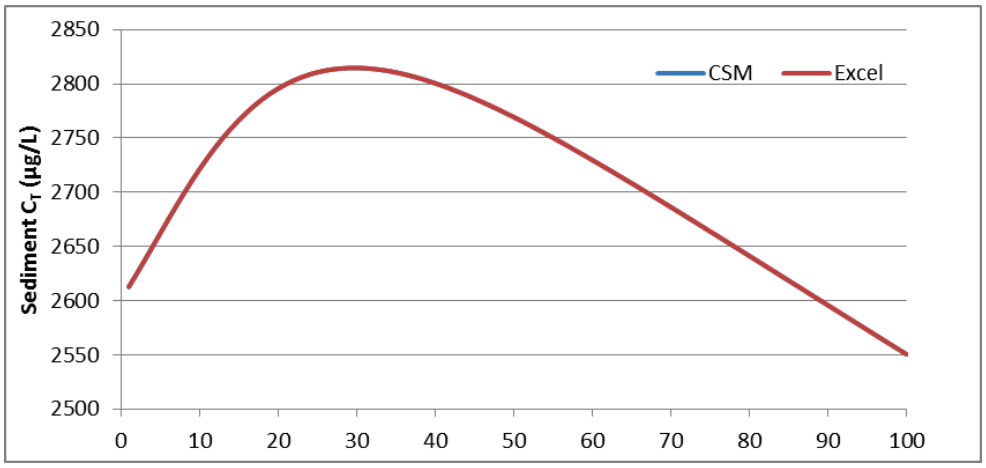

Figure 16. CSM and Excel computed total concentrations in the sediment layer.

Overall, these test cases further verify that algorithms and computer code computations were correctly implemented in CSM.

CONCLUSIONS: Aquatic contaminant simulation module (CSM) was developed for a variety of hydrologic and hydraulic models. The CSM simulates kinetic processes of contaminants in aquatic systems and interactions between the water column and sediment layer. The contaminants can be modeled in CSM through a range of user-specified chemical reactions as they are transported through the system. The contaminants can be defined to behave independently or can be coupled by being specified as part of a reaction (decay) chain. The contaminants can be modeled with multi-phases (dissolved, sorbed to DOC, algae, organic, and inorganic solids) under equilibrium or non-equilibrium portioning conditions.

Verification studies of the CSM were performed by comparing results with published, observed data sets and established model results generated from the RECOVERY and WASP for the same site conditions. CSM modeled the concentrations of DDE and lindane in water and upper sediment layer well when compared to measurements. The range of values calculated reflects the uncertainty in the

data used. In general, the model verifications with respect to temporal variations of multi-contaminants and multi-phase concentrations are satisfactory when compared with similar model results produced from RECOVERY and WASP. The ability of CSM to model a wide range of kinetic processes was validated and evaluated through a series of test cases. Once the CSM is fully integrated into HEC-RAS, additional testing and validation studies will be conducted in the future.

ACKNOWLEDGEMENT AND ADDITIONAL INFORMATION: This study was funded under the U.S. Army Environmental Quality Technology (EQT) Research Program. For additional information, contact: Dr. Zhonglong Zhang (601-634-3337, *zhonglong.zhang@erdc.dren.mil*) and Dr. Billy E. Johnson (601-634-3714, *billy.e.johnson@erdc.dren.mil*). This technical note should be cited as follows:

> Zhang, Z., and B.E. Johnson. 2016. *Verification and evaluation of aquatic contaminant simulation module (CSM)*. ERDC/TN EQT-16-2. Vicksburg, MS: U.S. Army Engineer Research and Development Center.

REFERENCES

Arnold, J.G., R. Srinivasan, R.S. Muttiah, and J.R. Williams. 1998. Large-area hydrologic modeling and assessment: Part I. Model development. *Journal of the American Water Resources Association* 34(1): 73-89.

Berger, R. C., J. N. Tate, G. L. Brown, and G. Savant. 2012. *Adaptive hydraulics user's manual: Guidelines for solving two-dimensional shallow water problems with the adaptive hydraulics modeling system*. Vicksburg, MS: U.S. Army Engineer Research and Development Center. *http://chl.erdc.usace.army.mil/Media/1/2/7/8/AdH_Manual-4.201.pdf*.

Boyer, J.M., S.C. Chapra, C.E. Ruiz, and M.S. Dortch. 1994. *RECOVERY, a mathematical model to predict the temporal response of surface water to contaminated sediments*. TR W-94-4. Vicksburg, MS: U.S. Army Engineer Waterways Experiment Station.

Di Toro, D. M., and P.R. Paquin. 1982. Time variable model of the fate of DDE and lindane in a quarry. *In Proceedings, Society of Environmental Toxicology and Chemistry 3rd Annual Meeting*, 14-17 November, Arlington, VA.

Freundlich, H. and H.S. Hatfield. 1926. Colloid and capillary chemistry. Methuen and Co. Ltd: London, England.

Hydrologic Engineering Center (HEC). 2010a. *HEC-RAS: River analysis system user's reference manual version 4.1*. Davis, California: U.S. Army Corps of Engineers Hydrologic Engineering Center.

Hydrologic Engineering Center (HEC). 2010b. HEC-RAS: *River analysis system hydraulic reference manual version 4.1*. Davis California: U.S. Army Corps of Engineers Hydrologic Engineering Center.

Langmuir, I. 1918. The adsorption of gases on plane surfaces of glass, mica, and platinum. *Journal of the American Chemical Society*, 40(9):1361-1403.

Neitsch, S.L., J.G. Arnold, J.R. Kiniry, and J.R. Williams. 2011. Soil and water assessment tool: Theoretical documentation, version 2009. TR-406. College Station, TX: Texas Water Resources Institute, Texas A&M University.

Ruiz, C.E., N.M. Aziz,.and Schroeder, P.R. 2000. *RECOVERY: A contaminated sediment-water interaction model*. ERDC/EL SR-D-00-1. Vicksburg, MS: U.S. Army Engineer Research and Development Center.

Wanner, O., T. Egli, T. Fleischmann, K. Lanz, P. Reichert, and R.P. Schwarzenbach. 1989. Behavior of the insecticides Disulfoton and Thiometon in the Rhine River: A chemodynamic study. *Environmental Science and Technology* 23(10):1232-1242.

Waybrant, R.C. 1973. Factors controlling the distribution and persistence of lindane and DDE in lentic environments. Ph.D. Thesis. Microfilm 256. Ann Arbor, MI: Purdue University.

Wool, T.A., R.B. Ambrose, J.L. Martin, and E.A. Comer. 2006. Water quality analysis simulation program (WASP) version 6.0 draft: User's manual. *http://www.epa.gov/athens/wwqtsc/html/wasp.html*.

Zhang, Z., and B. E. Johnson. 2016. *Aquatic contaminant and mercury simulation modules developed for hydrologic and hydraulic models*. ERDC/EL TR-16-X (in press). Vicksburg, MS: U.S. Army Engineer Research and Development Center.